Journal of Taibah University Medical Sciences (2023) 18(5), 1000–1010

Taibah University

Journal of Taibah University Medical Sciences

www.sciencedirect.com

Original Article

New flavone-based arylamides as potential *V600E-BRAF* inhibitors: Molecular docking, DFT, and pharmacokinetic properties

Abdullahi B. Umar, PhD * and Adamu Uzairu, PhD

Department of Chemistry, Faculty of Physical Sciences, Ahmad Bello University, Zaria, Kaduna State, Nigeria

Received 20 October 2022; revised 21 December 2022; accepted 21 February 2023; Available online 2 March 2023

الملخص

أهداف البحث: يعتبر بروتين كيناز "ب.ر.أ.ف.في-600إي" هدفا علاجيا جذابا وأساسيا في علاج سرطان الجلد وأنواع أخرى من الأورام. ومع ذلك، فإن مقاومته للمثبطات والآثار الجانبية المعروفة لبعض المثبطات المحددة تستلزم التحقيق في مثبطات جديدة وفعالة.

طريقة البحث: في العمل الحالي، تم استخدام استراتيجيات المحاكاة بالكمبيوتر مثل محاكاة الالتحام الجزيئي وحسابات نظرية الكثافة الوظيفية وتقييم الحرائك الدوائية، لتحديد مثبطات "ب.ر.أ.ف.في-600إي" المحتملة من مجموعة من 31 أريلاميدا جديدا مركبا قائما على الفلافون.

النتائج: أظهرت نتيجة الالتحام أن أربعة مركبات (10 ، 11 ، 28 ، 31) لديها درجات مقبولة. ظهرت النتيجة (-124.365 و -129.365 و -135.878 و -117.081 على التوالي) كأكثر مثبطات "ب.ر.أ.ف.في-600إي" نشاطا وفعالية والتي تصدرت فيمورافينيب. أثبت ظهور روابط الهيدروجين والتفاعلات الكارهة للماء مع المخلفات الأساسية لـ "ب.ر.أ.ف.في-600إي" الاستقرار العالي لهذه المجمعات. تم حساب الطاقة للمدارات الجزيئية الحدودية مثل أعلى مدار جزيئي مشغول وأدنى مدار جزيئي غير مشغول وفجوة الطاقة ومعلمات التفاعل الأخرى باستخدام نظرية الكثافة الوظيفية. تم فحص الأسطح المدارية الجزيئية الحدودية والإمكانات الكهروستاتيكية لإثبات توزيعات كثافة الشحنة التي قد تكون مرتبطة بالنشاط المضاد للسرطان. وبالمثل، كشفت المركبات المختارة عن خصائص دوائية فائقة وفقا لقواعد التشابه الدوائي (التوافر البيولوجي) وخصائص الحرائك الدوائية.

الاستنتاجات: وبالتالي، تم التعرف على المركبات المختارة كمرشحات قوية لـ "ب.ر.أ.ف.في-600إي" بخصائص حركية دوائية فائقة، ويمكن اقتراحها كعقاقير مرشحة واعدة للسرطان.

الكلمات المفتاحية: ب.ر.أ. ف-في. 600 .إي؛ أريلاميد؛ نظرية الكثافة الوظيفية؛ تشابه الأدوية

Abstract

Objectives: The V600E-BRAF protein kinase is an attractive and essential therapeutic target in melanoma and other tumors. However, because of its resistance to the known inhibitors and side effects of some identified inhibitors, new potent inhibitors need to be identified.

Methods: In the present work, in silico strategies such as the molecular docking simulation, DFT (Density-Functional-Theory) computations, and pharmacokinetic evaluation were used to determine potential V600E-BRAF inhibitors from a set of 31 synthesized novel flavone-based arylamides.

Results: The docking result demonstrated that four compounds (10, 11, 28, and 31) had acceptable docking scores (MolDock score of −167.523 kcal mol^{-1}, −158.168 kcal mol^{-1}, −160.581 kcal mol^{-1}, −162.302 kcal mol^{-1}, and a Rerank score of −124.365, −129.365, −135.878 and −117.081, respectively) appeared as most active and potent V600E-BRAF inhibitors that topped vemurafenib (−158.139 and −118.607 kcal mol^{-1}). The appearance of H-bonds and hydrophobic interactions with essential residues for V600E-BRAF proved the high stability of these complexes. The energy for the frontier molecular orbitals such as HOMO, LUMO, energy gap, and other reactivity parameters was computed using DFT. The frontier molecular-orbital surfaces and electrostatic potentials (EPs) were investigated to demonstrate the charge-density distributions that might be linked to anticancer activity. Similarly, the chosen compounds revealed superior pharmacological properties according to the drug-likeness rules (bioavailability) and pharmacokinetic properties.

* Corresponding author: Department of Chemistry, Faculty of Physical Sciences, Ahmad Bello University, Zaria, P.M.B.1045 Kaduna State, Nigeria.

E-mail: abdallahbum@gmail.com (A.B. Umar)

Peer review under responsibility of Taibah University.

ELSEVIER Production and hosting by Elsevier

 https://doi.org/10.1016/j.jtumed.2023.02.010

Conclusion: The chosen compounds were recognized as potent V600E-BRAF inhibitors with superior pharmacokinetic properties and could be promising cancer drug candidates.

Keywords: ADMET; Arylamide; DFT; Docking; Drug-likeness; *V600E-BRAF*

Introduction

BRAF is a protein kinase that plays a vital role in MAPK signaling pathways. *V600E-BRAF* is the most well-known mutation in *BRAF*; it was found in 8% of all the cancers, such as colorectal-cancer (10%), melanoma (60%), and thyroid cancer (30−70%).[1,2] Thus, the V600E-BRAF kinase is an important target in managing and treating cancer ailments.[3,4] Dabrafenib and vemurafenib are both inhibitors (selective) of V600E-BRAF that induce a highly effective automatic death of melanoma cells. They were endorsed by the US Food and Drug Administration (FDA) for the therapy of late-stage melanoma.[5,6] A single treatment with a V600E-BRAF inhibitor improved the patient's lifestyle and survival rate considerably. However, despite the approved V600E-BRAF inhibitors' success, resistance to these selective inhibitors emerged between 5 and 8 months of treatment.[7,8] The resistance developed to the selective V600E-BRAF inhibitors makes discovering and validating novel candidates an important line of research because it may lead to new treatments for V600E-BRAF-associated cancers. This approach requires a deep understanding of the heterogeneity of the tumor and the evolution of resistance. Furthermore, the identification and confirmation of lead compounds and the evaluation of active binding sites of bioactive targets linked with a specific lead compound require costly and time-consuming wet-lab activities.[9]

In silico strategies effectively decrease the time needed to acquire valuable drugs and reduce their accompanying financial costs, which makes them tempting low-cost approaches to find new potent and selective drugs.[10] Molecular docking is an outstanding in silico approach for filtering a huge chemical library to detect prospective chemicals that could be utilized to find a specific target's binding capacity. Over the last two decades, molecular docking has evolved as the model of structure-based virtual screening of several chemical databases.[11] It is extensively employed to select the most suitable alignment of a drug candidate in the active site of the protein and to predict its affinity. Previously, comprehensive docking investigations were performed to study the biological action of numerous chemical structures.[11−13] DFT is an extensive technique with a lower computational cost than several other approaches. DFT computations now produce the most reliable and accurate outcomes for various chemical systems that are well-matched with the experiments.[14] In silico drug-like and pharmacokinetics are additional (virtual) screening means for the approval of compounds that might demonstrate physiological drug-like ability. The procedures utilized to assess drug-likeness and pharmacokinetic properties are made from a combination of the experimental findings reported in several drug databases.[15]

Several approaches have been adopted to improve the existing anti-cancer drugs such as the formulation of nanomedicines.[16] Understanding the heterogeneity of the tumor and resistance of some known inhibitors is essential for the discovery of novel effective drugs for cancer. Arylamides were designed and employed as potent anticancer drugs acting on several targets and rarely with yet unidentified receptors. They are among the essential organic molecules containing different antimicrobial and anti-tumor potentials.[17,18] Flavones contain a class of natural products that can potentially become drugs.[19,20] Their anticancer potential includes numerous mechanisms of action, such as cell-cycle suppression, inhibition of several signaling pathways, autophagy induction, inhibition of calcium channels, and apoptosis.[21,22] In this investigation, a systematic computational investigation of thirty-one (31) new Flavone-based arylamides[23] was conducted using molecular docking simulation, DFT computations, and pharmacokinetic properties prediction. These compounds showed excellent activity on melanoma cells. The work aims to assess the anticancer potential of these chemical structures as likely drug candidates with desired properties.

Materials and Methods

Retrieval of compounds and optimization

Thirty-one series of Flavone-based arylamides were retrieved from the literature.[23] Structures of ligands were drawn employing ChemDraw (Table S1), and energy minimization was achieved using the MM2 force field in Spartan 14 to assist the docking program in detecting the bioactive conformer from the local minima. Optimization of the compounds was achieved using the DFT/B3LYP approach and 6−31G* basis-set.

Docking preparation and simulation

tThe protein Databank (http://www.rcsb.org/) was used to obtain the crystal structure of *V600E-BRAF* (PDB code: 3OG7)[24−26] and the native ligand (vemurafenib). The target was prepared by first extracting water molecules and detaching vemurafenib from the protein-ligand complex. Then, the native ligand was re-docked to the target to validate the molecular docking using Molegro Virtual-Docker (MVD) 6.0.[27] The active site of the target was determined automatically using a cavity detection package in MVD 6.0. The binding cavity of X: 1.59, Y: −1.28, Z: −6.2, and r: 28 Å was set with 0.30 Å resolution. The prepared structures with vemurafenib were imported into MVD, and 1500 iterations were set for the docking algorithm. The docking simulation was run at least 50 times for each of the ten poses, and the best poses were chosen based on predefined scoring functions.[28] Intermolecular interactions of the selected poses were visualized using Discovery-Studio (DS).

Table 1: Results of docking for the four best docked ligands in V600E-BRAF.

Complex	[a]MolDock score (kcal mol^{-1})	[b]Rerank-score	[c]E-inter (kcal mol^{-1})	[d]E−H bond (kcal mol^{-1})
10	−167.523	−124.365	−177.891	−3.979
11	−158.168	−129.365	−169.476	−5.842
28	−160.581	−135.878	−185.831	−4.387
31	−162.302	−117.081	−176.386	−5.010
Vem.	−158.139	−118.607	−167.952	−4.741

[a]Moldock score was obtained from the PLP scoring functions with a new H-bond term and extra chargeschemes [27]. [b]Rerank score is a linear combination of E-inter (Electrostatic, Van der Waals, H-bonding, steric) betweenthe ligand and the protein target, and E-intra. (Electrostatic, Van der Waals, H-bonding, sp2−sp2, torsion,)of the ligand weighted by pre-defined coefficients [27]. [c]E-inter is the total interaction energy between the protein and the pose. dE−H bond is H bond energy.

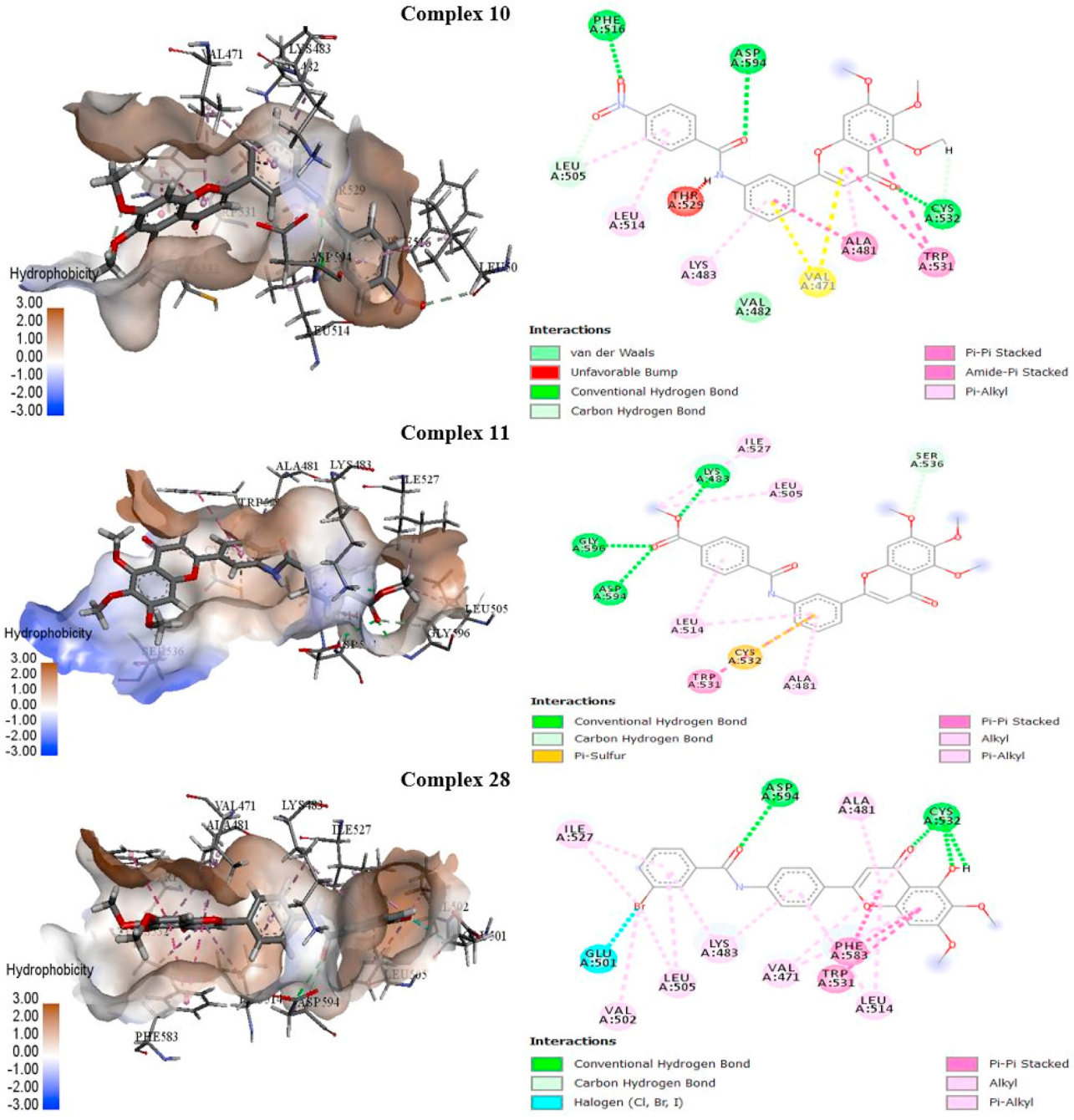

Figure 1: 3D and 2D models for the interactions of chosen complexes (10, 11, and 28).

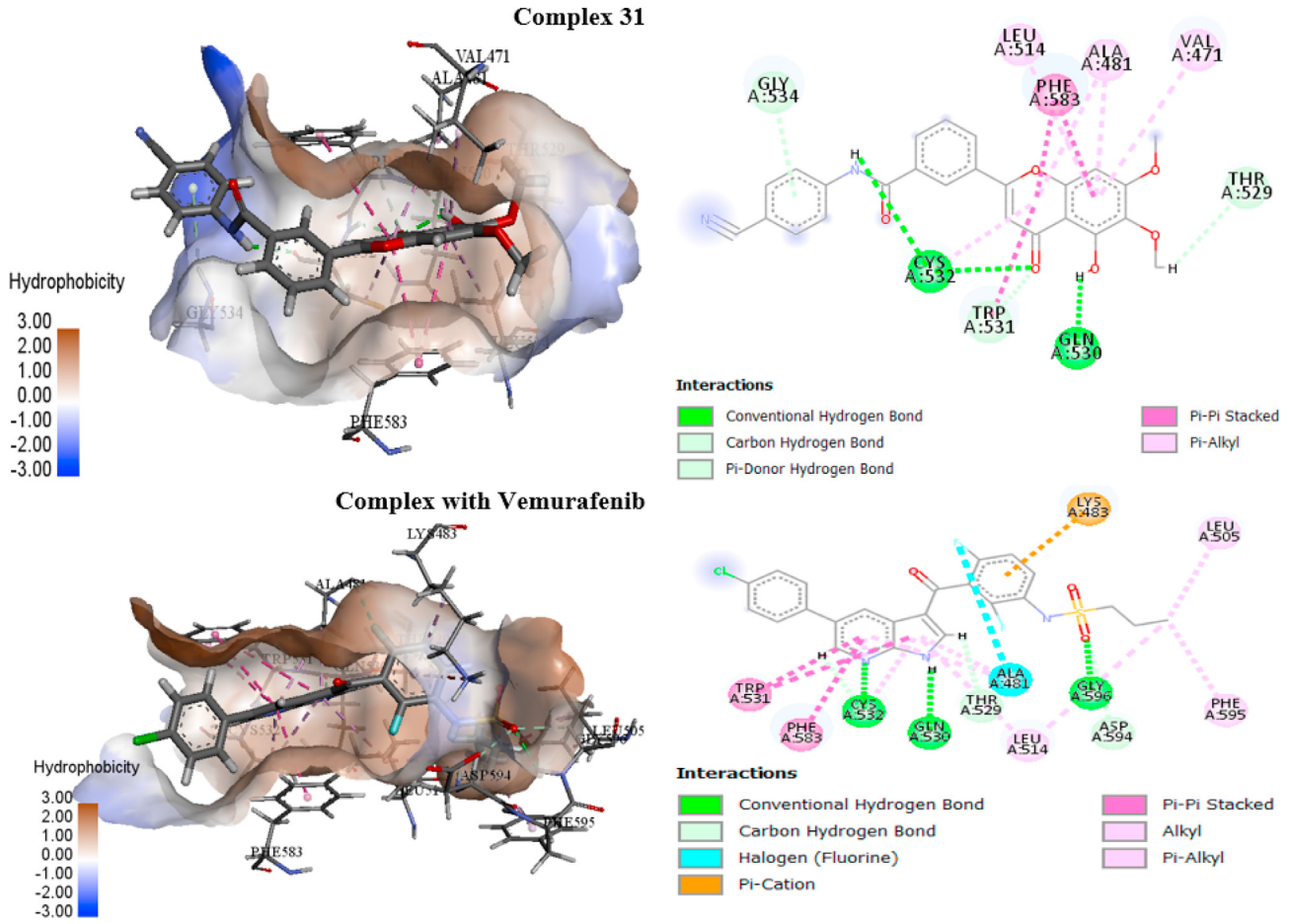

Figure 2: 3D and 2D models for the interactions of chosen complexes (3 1 and Vem.).

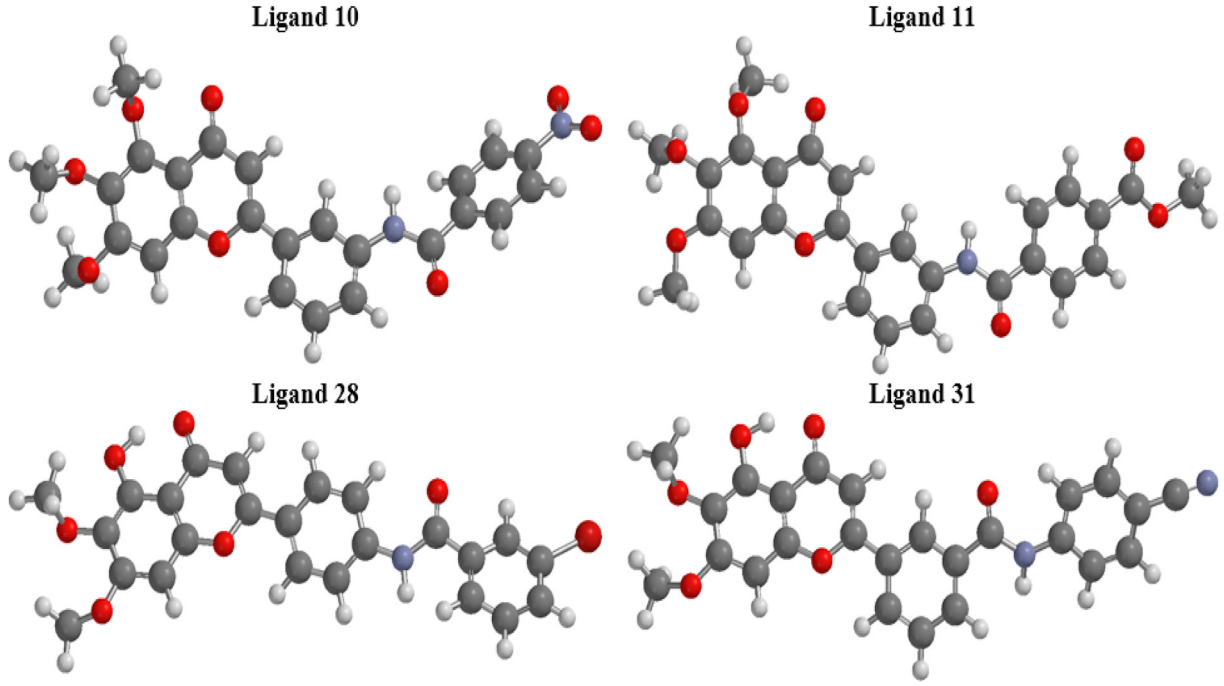

Figure 3: Optimized-geometric structures of the investigated ligands (10, 11, 28, and 31).

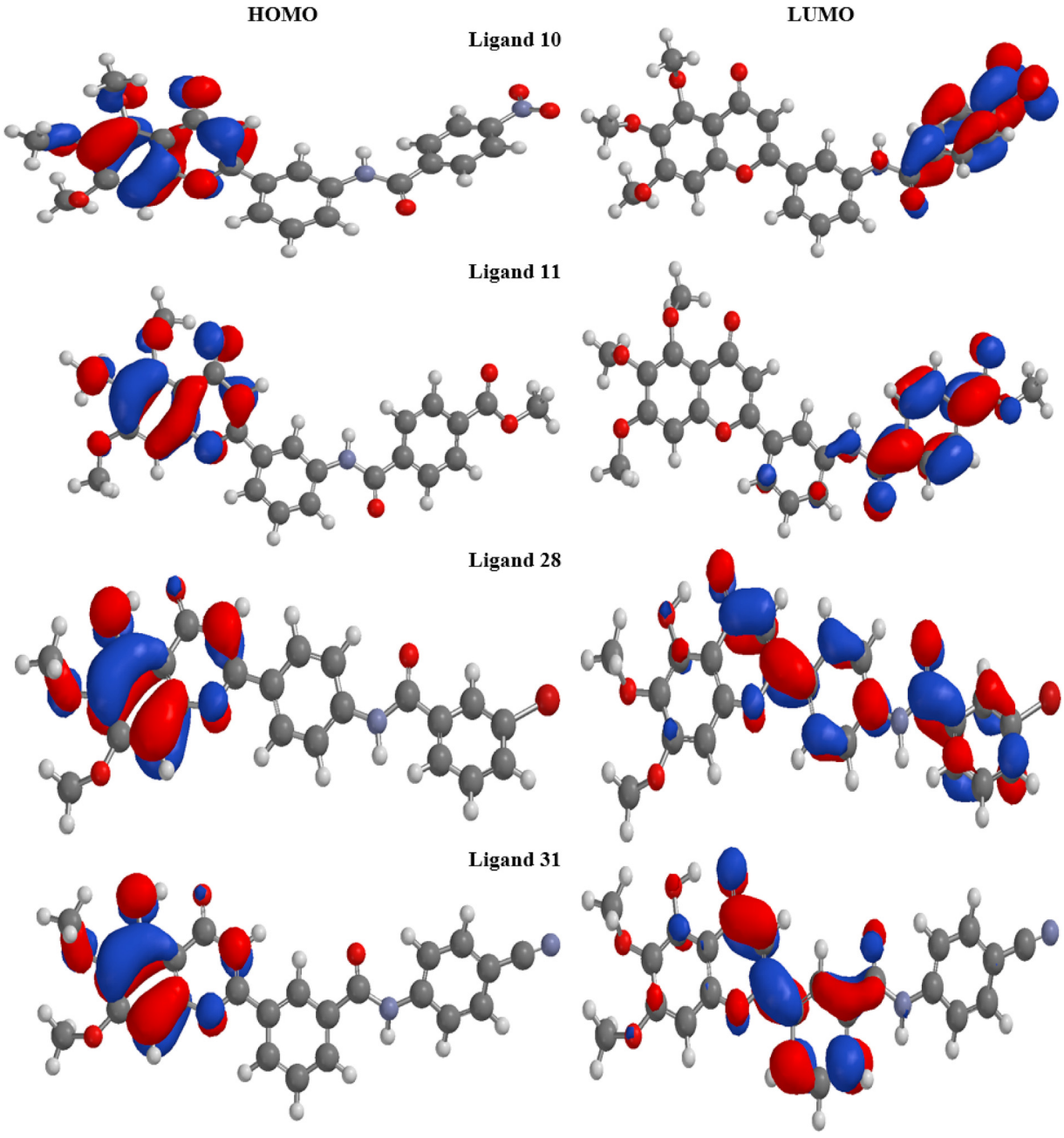

Figure 4: Frontier molecular-orbital surfaces of the investigated ligands (10, 11, 28, and 31).

Table 2: Frontier molecular-orbital energies and global-reactivity descriptors of the studied ligands.

S/N	E-HOMO (eV)	E-LUMO (eV)	ΔE	η	σ	χ	μ	ω
10	−6.21	−2.88	3.33	1.67	0.60	4.55	−4.55	6.20
11	−5.99	−2.00	3.99	2.00	0.50	4.00	−4.00	4.00
28	−5.8	−2.05	3.75	1.88	0.53	3.93	−3.93	4.11
3 1	−5.99	−2.26	3.73	1.87	0.54	4.13	−4.13	4.56

DFT computations

The structural and electronic properties for the four best compounds picked from the docking analysis were computed employing DFT/B3LYP and 6−31G* basis-set with Spartan 14. The parameters calculated in this investigation are the energies of the frontier molecular orbitals (HOMO, LUMO, and energy gap) and other reactivity parameters: chemical-hardness (η), softness (σ), electronegativity (χ) chemical potential (μ), and electrophilicity-index (ω).[29] In addition,

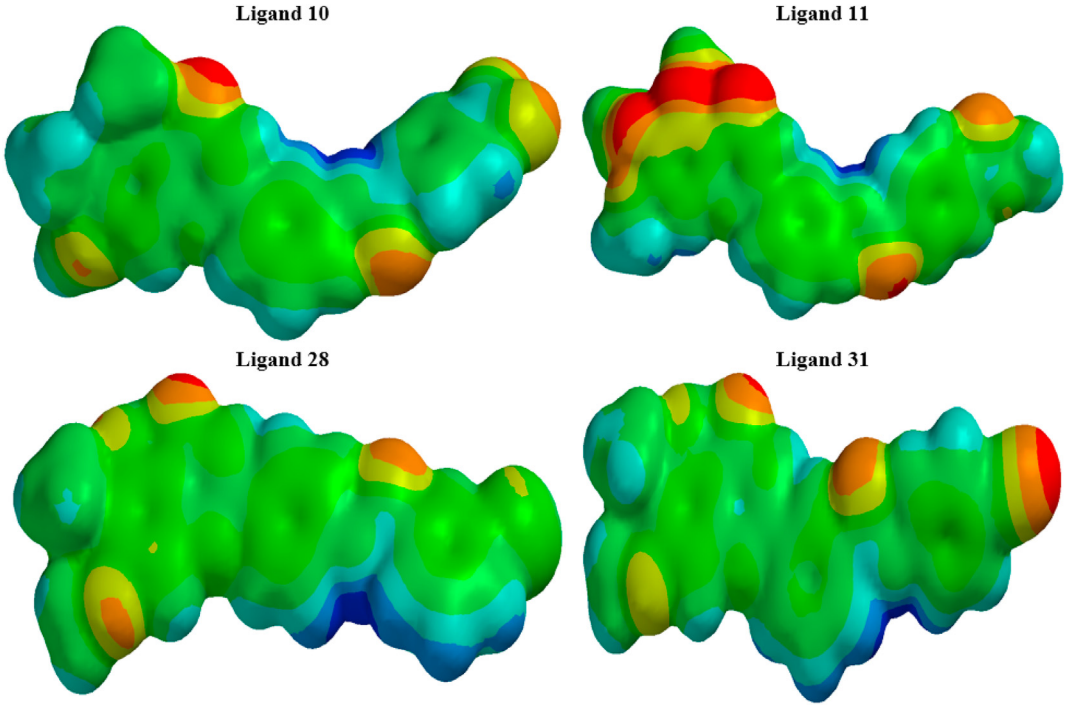

Figure 5: Electrostatic potential (EP) of the studied ligands (10, 11, 28, and 31).

Table 3: Predicted Drug-likeness parameters of the chosen ligands.

SN	Mol. wt.	HBA	HBD	Log P	TPSA (Å^2)	NRB	BA
10	476.43	8	1	3.76	132.82	8	0.55
11	489.47	8	1	3.78	113.30	9	0.55
28	496.31	6	2	4.85	98.00	6	0.55
31	442.42	7	2	3.87	121.79	6	0.55
Vem.	489.92	6	2	4.97	100.30	7	0.55

BA: bioavailability score.

the molecules' electrostatic potential surfaces (EPs) were achieved from the population-analysis computations and portrayed with Spartan 14. This plays an effective part in clarifying the importance of ligands/protein interaction in the active site of a target.

Drug-like and pharmacokinetic bio-chemical evaluation

SwissADME (www.swissadme.ch/), an online server, was used to investigate the drug-like behavior of the chosen compounds, and the pharmacokinetic parameters were examined using pkCSM (https://biosig.unimelb.edu.au/pkcsm//).

Results

The molecular docking results of the compounds, including vemurafenib, are given in Table S2. The superimposed alignment of the re-docked and original co-crystal ligand is presented in Figure S1. The complete docking results for the best four ligands and vemurafenib are presented in Table 1. Figures 1 and 2 depict the 3D and 2D interaction models of the selected docked ligands at the

Table 4: Predicted Pharmacokinetic properties of the chosen ligands.

	Absorption	Distribution			Metabolism							Excretion	Toxicity
					Substrate		Inhibitor						
					CYP								
SN	Absorption (% absorbed)	VDss (log L kg^{-1})	blood-brain barrier (BBB) (Log BB)	central nervous system (CNS) (Log PS)	2D6	3A4	1A2	2C 19 (yes/no)	2C9	2D6	3A4	Clearance (log mL min^{-1} kg^{-1})	Toxicity (yes/no)
10	100.00	−1.214	−0.943	−2.32	No	Yes	No	Yes	Yes	No	Yes	0.462	Yes
11	96.109	−0.628	−0.901	−3.14	No	Yes	No	Yes	Yes	No	Yes	0.535	No
28	100.00	−0.713	−0.761	−2.01	No	Yes	Yes	Yes	Yes	No	Yes	0.013	No
31	89.488	−0.557	−0.742	−2.143	No	Yes	Yes	Yes	Yes	No	Yes	0.423	No
Vem.	98.853	−0.445	−1.647	−3.463	No	Yes	No	Yes	Yes	No	Yes	0.132	No

V600E-BRAF binding site. Table S3 presents the types of interactions in each selected complex. The Optimized geometries and the frontier molecular orbitals (HOMO and LUMO illustrations) of the selected ligands achieved from DFT computations are given in Figures 3 and 4. Table 2 shows the quantum descriptors, while Figure 5 depicts the studied ligands' electrostatic potential (EP) surfaces. Their drug-likeness and pharmacokinetics were determined to confirm further that the chosen compounds are possible drugs. The predicted drug-likeness and pharmacokinetic properties are given in Tables 3 and 4.

Discussion

The most potent inhibitors were identified by docking all the 31 studied ligands including Vemurafenib into the binding pocket of the *V600E-BRAF* target. Before the docking was performed for the whole data, the docking method was authenticated through a re-docking technique. Thus, the Vemurafenib (co-crystallized) was re-docked at the exact site where the co-crystal ligand was initially bound with *V600E-BRAF* kinase. Re-docking of vemurafenib at the V600E-BRAF kinase receptor revealed an RMSD value of 1.413 Å that satisfied the validity standards of RMSD value <2.0 Å.[30] Hence, the docking procedure using MVD has acceptable precision in repositioning vemurafenib at the V600E-BRAF active sites. The super-imposed alignment of the re-docked and actual co-crystal is portrayed in Figure S1. The coordinates for the active site and the grid-box size employed in the established re-docking procedure were also adopted for docking the studied compounds. The top inhibitors of V600E-BRAF were sorted according to the docking score compared to vemurafenib[31] , and the chosen ligand binds efficiently to the target.

The identification of the main residues responsible for the inhibition of *V600E-BRAF* inside the binding pocket for the four chosen complexes (10, 11, 28, and 31) was achieved by employing the DS Visualizer. The potency of the interaction between the ligand and protein was assessed by the Rerank score. From the docking result, the protein-ligand interactions demonstrated that the existence of methoxy groups, chromen, and N-phenyl benzamide moieties in the structures played a vital role. The complete docking results for the best four ligands and vemurafenib are presented in Table 1. Figures 1 and 2 depict the 3D and 2D interaction models of the selected docked poses in the binding site of V600E-BRAF. Table S3 presents the interaction types involved in each of the chosen complexes. The chosen ligands developed bonds, and non-bond interaction at the binding pocket of the *V600E-BRAF* target, as indicated by the inter-energy and H-bonding energy (Table 1). They all have a MolDock-score <-90 kcal mol^{-1}, which shows their potential to bind the target protein efficiently.[32] The complex structures of the four best poses based on the docking scores are discussed in detail below as presented (Figures 1 and 2).

The complex structure of the docked compound-10 with the target is shown in Figure 1 (complex 10). A MolDock-score of -167.523 kcal mol^{-1} and a Rerank score of -124.365 was observed. The E−H bond was -3.979 kcal mol^{-1} (Table 1). The good docking scores suggest the potential for good interactions between this compound and the protein. The binding mode observed in Figure 1 (complex 10) indicated that compound 10 established interactions through H-bonding with the backbone of the center amino acid-residues: PHE516, CYS532, and1ASP594; and showed a favorable π−π interaction with TRP531, ALA481, and VAL482 residues, which are important interactions for selectivity.[23] In addition, compound 10 formed π-alkyl interactions with LEU505, LEU514, VAL471, ALA481, and LYS483 at the binding cavity and a C−H bond to the side chain of LEU505 and CYS532 of the center area, in a similar pattern reported in the literature.[11]

Compound 11 docked on the V600E-BRAF target revealed a MolDock and Rerank score of -158.168 and -129.365 kcal mol^{-1}. The H-bond energy was -5.842 kcal mol^{-1} (Table 1). The acceptable docking scores for the complex resulted from the three conventional H-bonds, two C−H bonds formed, and other hydrophobic interactions, which conveys stabilizing charges probable for intercalating the molecule in the V600E-BRA as illustrated in Figure 1 (complex 11). The docking mode portrayed in complex 11 indicated an interaction network with the residues, including π-alkyl with LEU514 (2) and ALA481; π-sulfur with CYS532; H-bonding with LYS483, ASP59, and GLY596; C−H interaction with SER536 and GLY596 and π−π with TRP531. The binding pattern and the residues involved are similar to those on the same target reported by Umar et al.[33]

Compound-28 docked inside the active site of V600E-BRAF as shown by complex 28 in Figure 1. The excellent docking score for the complex showed the likelihood of steady and useful interactions between this ligand and the V600E-BRAF (Table 1). There were four conv. H bond between the ligand and V600E-BRAF; CYS532 (2) and ASP594 and one C−H bond with ASP594 as indicated by complex 28 (Figure 1). Three alkyl interactions were formed between compound-28 and the protein, namely VAL502, LEU505, and ILE527. The strength of the complex could be linked to π-alkyl interactions (LEU505, CYS532, LYS483, ILE527, VAL471, ALA481, LEU514, and VAL471) and π−π type of interactions to TRP531 and PHE583 (2) comparable to vemurafenib (Figures 1 and 2). The complex showed a similar pattern to the literature[34] on the same target.

The mode of binding for compound-31 on the V600E-BRAF is given in Figure 2 (complex 31). A MolDock and Rerank score of -162.302 and -117.081 kcal mol^{-1} and E−H bond of -5.010 kcal mol^{-1} were observed as given in Table 1. The binding mode for compound-31 on the *V600E-BRAF* was given in Figure 2 (complex 31). A MolDock, Rerank-score of -162.302 kcal mol^{-1} and -117.081 and E-Hbond of -5.010 kcal mol^{-1} were observed as given in Table 1. The binding mode displayed in Figure 2, revealed that compound 31 established interactions through H-bond with the back-bone of the central residues CYS532 (2) and GLN530; and showed a C-H interaction with the side chain of TRP531, THR529, and GLY534. The strength of the complex could be connected to an additional, π-alkyl interaction with (ALA481, CYS532, VAL471, ALA481, and LEU514) and a promising π-π interaction with PHE583 (2) and TRP531 similar to Vemurafenib (Figure 2). These binding-mode predicted might offer an

understanding of interactions that may be influence the detected inhibition of *V600E-BRAF* by the studied ligand and thus might help to develop better inhibitors.

The H bond is a unique sign of robust protein and ligand interactions and typically results in high binding affinity.[35] In such interactions, the number of H bonds usually boosts the inhibitor potential on the target; Figures 1 and 2 show 3D and 2D models of the interaction modes in the target binding site—the conv. The H bonds of the chosen ligands with anticancer receptors resulted in a suitable ligand binding. Again, as a standard comparison with the investigated ligands, vemurafenib was docked into the same examined protein, and all the chosen ligands surpassed vemurafenib. Interestingly, the investigated ligands inhibited the melanoma target better than vemurafenib. In addition, the chosen ligands had higher docking scores than vemurafenib.

The geometry-optimized structures of the selected ligands from DFT computations indicated that all the geometry-optimized structures conform to a global minimum (Figure 3). The frontier molecular orbitals (HOMO and LUMO) of the four best ligands determine a vital role in charge−transfer interactions between the ligand and the target's active site. As illustrated in Figure 4, the blue and red colors reveal the positive and negative regions of the orbital.[36] Additionally, the shapes of the frontier orbitals can be employed as a guide in determining reactivity. In every ligand, the HOMO is delocalized onto the chromen ring and largely dominated by the pi-bonds. By pattern, the blue area denotes the highest value of HOMO, while the red area denotes the lowest value.[37] The HOMO electron-density distribution of the investigated ligands demonstrates promising interactions of the ligands to V600E-BRAF. Similarly, the LUMO delocalizes over several areas of the aryl ring for ligands 10 and 11. As for ligands 28 and 31, the enormous contribution arrives from the conjugated bonds of the flavone ring. The HOMO and LUMO electronic surfaces displayed that the flavone and the aryl rings can interact with the target under good circumstances. The frontier molecular orbitals (HOMO and LUMO) of the five best ligands indicated a crucial role in charge transfer interactions between the ligand and the target's active site.

Table 2 displays the energies of HOMO and LUMO, including quantum chemical descriptors associated with the studied ligands. A good electron-donor molecule has a high HOMO energy, whereas a lower energy value indicates a weak electron-acceptor.[38] Also, a lower energy gap (LUMO−HOMO) significantly affects intermolecular charge transfer and molecule bioactivity. As a result, a small energy gap observed in the hit ligands positively affects the electron's movement from the HOMO to the LUMO, resulting in a strong affinity of the inhibitor for V600E-BRAF. The Egap value rises in accordance with the following: 10 (3.33 eV) > 31 (3.73 eV) > 28 (3.75 eV) > 11 (3.99 eV). Consequently, the reactivity order improves accordingly, where the most reactive is 110 (3.33 eV). The order of reactivity increases fits the reductions in energy-gap values.

The η (hardness) and the σ (softness) are significant reactivity variables for the performance of a ligand in a chemical system. Hard molecules always have a higher resistance to altering their electronic dispersal during a chemical reaction. In comparison, soft molecules have a lower resistance to altering the distribution of their electrons in a reaction.[39,40] Results from Table 2 indicated a high η value with a low σ value compared to analogous reported molecules.[41] The χ (electronegativity) of a given molecule determines its capacity for electron attraction.[42] The χ was computed at 3.93−4.55 eV, labeling the selected ligands as donor electrons. The μ (chemical potential) specifies negative values for all the studied ligands, suggesting good strength and establishing a stable complex. A molecule's ω (electrophilicity) predicts the electrophilic nature and measures the tendency to accept an electron. The position of organic molecules based on the ω values follows the order; $\omega < 0.8$ eV indicates weak electrophiles, ω between 0.8 and 1.5 eV, indicates moderate electrophiles, and $\omega > 1.5$ eV, reveals strong electrophiles.[43] The computed ω describes the studied ligands as good electrophiles. It has been reported that ligands with a high ω value have potential anticancer activities.[44] Finally, comparing the orbital energies (eV), global-reactivity variables, and docking scores of the best four ligands from the dataset, the selected ligands may be considered potential V600E-BRAF inhibitors with desired properties.

The molecular electrostatic potential (MEP) surface designates the charge distribution, thus providing a good understanding of the physical and chemical properties of a molecule. It predicts a molecule's electrophilic and nucleophilic active sites.[45] When the point of charge is located in the surplus positive charge area, the point charge ligand interaction becomes repulsive, and the electrostatic potential will therefore be positive. But, if the point of charge is situated in a region of a surplus negative charge, there is an attractive interaction, and the EPs becomes negative.[46,47] The MEP maps of the chosen ligands are presented in Figure 5. From the map, the red color shows the nucleophilic region, the blue color portrays the electrophilic region, and the colors in-between indicate the middle values of the MEP. Thus, the increase in possible follows the order: red < orange < yellow < green < blue.[36] In most cases, the negative charges are situated on the O-atoms, and the positive areas of the molecules are the areas where the H-atoms bonded to the O-atoms are situated. The positive and negative cores of the chosen molecules form interactions with both the bonded and non-bonded (particularly H-bonds) in the complexes during the docking.[46]

Drug-likeness and pharmacokinetic investigations for the investigated ligands were achieved through SwissADME and pkCSM web servers.[48,49] Lipinski's rule[50] suggests that good absorption occurs only when the mol. wt. <500, H bond-donors < 5, log P < 5, H bond-acceptors < 10. Table 3 results revealed that the mol. wt. of the researched compounds are 496.31 to 442.42 g mol^{-1}; therefore, the chosen compounds are within the permissible range of the Lipinski rule. None of the studied compounds have more than 10 H-bond acceptors. The highest number was observed at eight for ligands 10 and 11. It was also observed that the selected ligands have fewer than 5 H-bond donors. The value for log P was <5 for all the selected ligands. Ghose suggests that the log P value for a given ligand should be in the range of −0.4 to 5.6. In this study, the log P value for all the selected compounds was 3.87 to 3.76. Veber's rule[51] recommends that the TPSA should not be 140 $Å^2$ and that

the TPSA of the selected ligands was not >132.82 Å^2. Veber and Mugge's rules[52] propose that NRB in the ligand should not be >10 and 15. According to the results in Table 3, all the ligands examined in this study have the highest of 9 (RB).[51,52] The selected ligands were further filtered for an optimum profile of permeability and bioavailability utilizing bioavailability score (ABS) standards. An ABS score of 0.55 implies compliance with the Lipinski rule.[50]

The intestinal absorbance of the selected ligands has a value of 89.488−100%, demonstrating their ease of absorption. VDss indicates a volume distribution at a stable state, which indicates a uniform distribution of the drug to all the tissues at sufficient time. A VDss-value >0.5 suggests that a drug candidate is sufficiently spread in the plasma, while a value below −0.5 signifies that the drug has a low capacity to cross over to the cell membrane. The indicated VDss is in the range of −0.557 to −1.214, which implies that the investigated ligands have proper distribution in plasma. Also, the BBB (blood−brain barrier) and the penetrability to the CNS (central nervous system) are essential factors in acquiring the optimum pharmacological drug. According to the standard scale of the drug, the BBB and CNS penetrability standard values are shown as <−1 to >0.3 for log BB and <−3 to >−2 for log PS. In a given ligand, the log BB of <−1 exhibits the insufficient diffusion of the drug molecule to the brain, whereas log BB-value of >0.3 indicates that the drug molecule can cross the BBB, and log PS-value of >−2 means that the drug molecule can enter the CNS, while <−3 suggests that it will be hard for the drug molecule to make it to the CNS.[53] Table 4 shows that the chosen ligands have demonstrated a high possibility of crossing the barriers.

Cytochrome (CYP450) is a robust metabolic enzyme in the body of a human with five main isoforms: CYP A2, CYP2 C19, CYP2 C9, CYP2 D6, and CYP3 A4. Results in Table 4 show a promising enzyme inhibition capacity and hence safe pharmacokinetic interactions. The clearance determines the dosing effect and bioavailability of a drug to reach the required concentrations. A low clearance value suggests increased endurance of a drug molecule in the body. All the chosen ligands demonstrated good acceptability in the body. Toxicity is used to decide whether a drug candidate is toxic or not. From Table 4, ligands 11, 28, and 31 are non-toxic. Consequently, the chosen ligands have the preferred pharmacokinetic properties and can be used as V600E-BRAF inhibitors.

Conclusions

Molecular docking simulation, DFT computations, and pharmacokinetic evaluation were successfully used in this research to determine potential hits against V600E-BRAF from a series of novel Flavone-based arylamides. Four top-ranked compounds (10, 11, 28, and 31) were selected as their docking scores were higher than vemurafenib in the active site of the V600E-BRAF target. According to the docking results, the interactions of the hydrophobic and H bonds play a significant role in the binding interactions of the potential compounds and the V600E-BRAF. The quantum chemical parameters computed using the DFT approach recognized the selected molecules as steady structures and highly electrophilic. At the same time, the distribution of the MEP identified the potential sites for the nucleophilic and electrophilic attacks. The predicted physicochemical and pharmacokinetic parameters were in the acceptable range of drug screening criteria. It is clear from the broad computational investigations that compounds (11, 28, and 31) may be considered potential hits against the V600E-BRAF target and are likely to have promising action as anticancer agents.

Source of funding

This work was fully sponsored by the Tertiary Education Trust Fund (TETFUND) with the grant number: TETF/DR&D/UNI/ZARIA/IBR/2020/VOL./54.

Conflict of interest

The authors have no conflict of interest to declare.

Ethical approval

This research was fully sponsored by the Tertiary Education Trust Fund (NG) under IBR Project Grant 2020 with project number (TETF/DR&D/UNI/ZARIA/IBR/2020/VOL./54).

Consent

Not relevant.

Authors' contribution

ABU: Designed and performed the study, interpreted the results, and wrote the manuscript. AU: Contributed to designing the study and supervised and edited the manuscript. All authors have critically reviewed and approved the final draft and are responsible for the content and similarity index of the manuscript.

Acknowledgment

Thanks to the TETFUND for the 2020 IBR (Institution-Based-Research) Project Grant (TETF/DR&D/UNI/ZARIA/IBR/2020/VOL.1/54) granted for this study.

Appendix A. Supplementary data

Supplementary data to this article can be found online at https://doi.org/10.1016/j.jtumed.2023.02.010.

References

1. Amin KM, El-Badry OM, Rahman DEA, Ammar UM, Abdalla MM. Design, synthesis, anticancer evaluation and molecular docking of new V600EBRAF inhibitors derived from pyridopyrazinone. **Eur J Chem 2016**; 7(1): 19−29.
2. Prahallad A, Sun C, Huang S, Di Nicolantonio F, Salazar R, Zecchin D, et al. Unresponsiveness of colon cancer to BRAF (V600E) inhibition through feedback activation of EGFR. **Nature 2012**; 483(7387): 100−103.

3. Akhtar MJ, Siddiqui AA, Khan AA, Ali Z, Dewangan RP, Pasha S, et al. Design, synthesis, docking and QSAR study of substituted benzimidazole linked oxadiazole as cytotoxic agents, EGFR and erbB2 receptor inhibitors. **Eur J Med Chem 2017**; 126: 853–869.
4. Regad T. Targeting RTK signaling pathways in cancer. **Cancers 2015**; 7(3): 1758–1784.
5. Wilhelm SM, Adnane L, Newell P, Villanueva A, Llovet JM, Lynch M. Preclinical overview of sorafenib, a multikinase inhibitor that targets both Raf and VEGF and PDGF receptor tyrosine kinase signaling. **Mol Cancer Ther 2008**; 7(10): 3129–3140.
6. Bryan MC, Falsey JR, Frohn M, Reichelt A, Yao G, Bartberger MD, et al. N-substituted azaindoles as potent inhibitors of Cdc7 kinase. **Bioorg Med Chem Lett 2013**; 23(7): 2056–2060.
7. Flaherty KT, Puzanov I, Kim KB, Ribas A, McArthur GA, Sosman JA, et al. Inhibition of mutated, activated BRAF in metastatic melanoma. **N Engl J Med 2010**; 363(9): 809–819.
8. Infante J, Fecher L, Nallapareddy S, Gordon M, Flaherty K, Cox D, et al. Safety and efficacy results from the first-in-human study of the oral MEK 1/2 inhibitor GSK1120212. **J Clin Oncol 2010**; 28(15_suppl). 2503–2503.
9. Karthick T, Tandon P. Computational approaches to find the active binding sites of biological targets against busulfan. **J Mol Model 2016**; 22(6): 1–9.
10. Cumming JG, Davis AM, Muresan S, Haeberlein M, Chen H. Chemical predictive modelling to improve compound quality. **Nat Rev Drug Discov 2013**; 12(12): 948–962.
11. Umar AB, Uzairu A, Shallangwa GA, Uba S. Molecular docking strategy to design novel V600E-BRAF kinase inhibitors with prediction of their drug-likeness and pharmacokinetics ADMET properties. **Chem Afr 2020**: 1–17.
12. Deghady AM, Hussein RK, Alhamzani AG, Mera A. Density functional theory and molecular docking investigations of the chemical and antibacterial activities for 1-(4-hydroxyphenyl)-3-phenylprop-2-en-1-one. **Molecules 2021**; 26(12): 3631.
13. Hussein R, Elkhair H. Molecular docking identification for the efficacy of some zinc complexes with chloroquine and hydroxychloroquine against main protease of COVID-19. **J Mol Struct 2021**; 1231:129979.
14. Umar BA, Uzairu A. In-silico approach to understand the inhibition of corrosion by some potent triazole derivatives of pyrimidine for steel. **SN Appl Sci 2019**; 1(11): 1413.
15. Opo FA, Rahman MM, Ahammad F, Ahmed I, Bhuiyan MA, Asiri AM. Structure based pharmacophore modeling, virtual screening, molecular docking and ADMET approaches for identification of natural anticancer agents targeting XIAP protein. **Sci Rep 2021**; 11(1): 1–17.
16. Elnaggar MH, Abushouk AI, Hassan AH, Lamloum HM, Benmelouka A, Moatamed SA, et al. Nanomedicine as a putative approach for active targeting of hepatocellular carcinoma. In: *Seminars in cancer biology*. Elsevier; 2019.
17. Landucci E, Gencarelli M, Mazzantini C, Laurino A, Pellegrini-Giampietro DE, Raimondi L. N-(3-Ethoxy-phenyl)-4-pyrrolidin-1-yl-3-trifluoromethyl-benzamide (EPPTB) prevents 3-iodothyronamine (T1AM)-induced neuroprotection against kainic acid toxicity. **Neurochem Int 2019**; 129:104460.
18. Vu HN, Kim JY, Hassan AH, Choi K, Park J-H, Park KD, et al. Synthesis and biological evaluation of picolinamides and thiazole-2-carboxamides as mGluR5 (metabotropic glutamate receptor 5) antagonists. **Bioorg Med Chem Lett 2016**; 26(1): 140–144.
19. Zhao L, Yuan X, Wang J, Feng Y, Ji F, Li Z, et al. A review on flavones targeting serine/threonine protein kinases for potential anticancer drugs. **Bioorg Med Chem 2019**; 27(5): 677–685.
20. Verma AK, Pratap R. The biological potential of flavones. **Nat Prod Rep 2010**; 27(11): 1571–1593.
21. Zhang X, Li H, Zhang H, Liu Y, Huo L, Jia Z, et al. Inhibition of transmembrane member 16A calcium-activated chloride channels by natural flavonoids contributes to flavonoid anticancer effects. **Br J Pharmacol 2017**; 174(14): 2334–2345.
22. Borah N, Gunawardana S, Torres H, McDonnell S, Van Slambrouck S. 5, 6, 7, 3′, 4′, 5′-Hexamethoxyflavone inhibits growth of triple-negative breast cancer cells via suppression of MAPK and Akt signaling pathways and arresting cell cycle. **Int J Oncol 2017**; 51(6): 1685–1693.
23. Hassan AH, Lee K-T, Lee YS. Flavone-based arylamides as potential anticancers: design, synthesis and in vitro cell-based/cell-free evaluations. **Eur J Med Chem 2020**; 187:111965.
24. Brose MS, Volpe P, Feldman M, Kumar M, Rishi I, Gerrero R, et al. BRAF and RAS mutations in human lung cancer and melanoma. **Cancer Res 2002**; 62(23): 6997–7000.
25. Bollag G, Hirth P, Tsai J, Zhang J, Ibrahim PN, Cho H, et al. Clinical efficacy of a RAF inhibitor needs broad target blockade in BRAF-mutant melanoma. **Nature 2010**; 467(7315): 596.
26. Choi W-K, El-Gamal MI, Choi HS, Baek D, Oh C-H. New diarylureas and diarylamides containing 1, 3, 4-triarylpyrazole scaffold: synthesis, antiproliferative evaluation against melanoma cell lines, ERK kinase inhibition, and molecular docking studies. **Eur J Med Chem 2011**; 46(12): 5754–5762.
27. Molegro A. *MVD 5.0 Molegro virtual docker. DK-8000 Aarhus C, Denmark*; 2011.
28. Thomsen R, Christensen MH. MolDock: a new technique for high-accuracy molecular docking. **J Med Chem 2006**; 49(11): 3315–3321.
29. Tsuneda T, Song J-W, Suzuki S, Hirao K. On Koopmans' theorem in density functional theory. **J Chem Phys 2010**; 133(17):174101.
30. Yusuf D, Davis AM, Kleywegt GJ, Schmitt S. An alternative method for the evaluation of docking performance: RSR vs RMSD. **J Chem Inf Model 2008**; 48(7): 1411–1422.
31. Umar AB, Uzairu A, Shallangwa GA, Uba S. *Molecular Docking Strategy to Design Novel V600E-BRAF Kinase Inhibitors with Prediction of Their Drug-Likeness and Pharmacokinetics ADMET Properties*. **Chemistry Africa 2020**: 1–17.
32. Abdullahi M, Uzairu A, Shallangwa GA, Arthur DE, Umar BA, Ibrahim MT. Virtual molecular docking study of some novel carboxamide series as new anti-tubercular agents. **Eur J Chem 2020**; 11(1): 30–36.
33. Umar AB. In silico studies of some potential anti-cancer agents on M19-MEL cell line. **Moroc J Chem 2021**; 9(2).
34. Umar AB, Uzairu A, Shallangwa GA, Uba S. Docking-based strategy to design novel flavone-based arylamides as potent V600E-BRAF inhibitors with prediction of their drug-likeness and ADMET properties. **Bull Natl Res Cent 2020**; 44(1): 1–11.
35. Khan IM, Islam M, Shakya S, Alam N, Imtiaz S, Islam MR. Synthesis, spectroscopic characterization, antimicrobial activity, molecular docking and DFT studies of proton transfer (H-bonded) complex of 8-aminoquinoline (donor) with chloranilic acid (acceptor). **J Biomol Struct Dyn 2021**: 1–15.
36. Balachandran V, Karpagam V, Revathi B, Kavimani M, Ilango G. Conformational stability, spectroscopic and computational studies, HOMO–LUMO, NBO, ESP analysis, thermodynamic parameters of natural bioactive compound with anticancer potential of 2-(hydroxymethyl) anthraquinone. **Spectrochim Acta Mol Biomol Spectrosc 2015**; 150: 631–640.
37. Celik S, Akyuz S, Ozel AE. Structural and vibrational investigations and molecular docking studies of a vinca alkoloid, vinorelbine. **J Biomol Struct Dyn 2022**: 1–20.
38. Manoj K, Elangovan N, Chandrasekar S. Synthesis, XRD, hirshfeld surface analysis, ESP, HOMO-LUMO, quantum chemical modeling and anticancer activity of di (p-methyl

benzyl)(dibromo)(1, 10-phenanthroline) tin (IV) complex. **Inorg Chem Commun 2022**; 139:109324.
39. Murulana LC, Singh AK, Shukla SK, Kabanda MM, Ebenso EE. Experimental and quantum chemical studies of some bis (trifluoromethyl-sulfonyl) imide imidazolium-based ionic liquids as corrosion inhibitors for mild steel in hydrochloric acid solution. **Ind Eng Chem Res 2012**; 51(40): 13282−13299.
40. Wazzan NA. DFT calculations of thiosemicarbazide, aryliso-thiocynates, and 1-aryl-2, 5-dithiohydrazodicarbonamides as corrosion inhibitors of copper in an aqueous chloride solution. **J Ind Eng Chem 2015**; 26: 291−308.
41. Fahim AM, Farag AM. Synthesis, antimicrobial evaluation, molecular docking and theoretical calculations of novel pyrazolo [1, 5-a] pyrimidine derivatives. **J Mol Struct 2020**; 1199: 127025.
42. Karton A, Spackman PR. Evaluation of density functional theory for a large and diverse set of organic and inorganic equilibrium structures. **J Comput Chem 2021**; 42(22): 1590−1601.
43. Edim MM, Enudi OC, Asuquo BB, Louis H, Bisong EA, Agwupuye JA, et al. Aromaticity indices, electronic structural properties, and fuzzy atomic space investigations of naphthalene and its aza-derivatives. **Heliyon 2021**; 7(2):e06138.
44. Srivastava R. Theoretical studies on the molecular properties, toxicity, and biological efficacy of 21 new chemical entities. **ACS Omega 2021**; 6(38): 24891−24901.
45. Mıhçıokur Ö, Özpozan T. Molecular structure, vibrational spectroscopic analysis (IR & Raman), HOMO-LUMO and NBO analysis of anti-cancer drug sunitinib using DFT method. **J Mol Struct 2017**; 1149: 27−41.
46. Jordaan MA, Ebenezer O, Damoyi N, Shapi M. Virtual screening, molecular docking studies and DFT calculations of FDA approved compounds similar to the non-nucleoside reverse transcriptase inhibitor (NNRTI) efavirenz. **Heliyon 2020**; 6(8):e04642.
47. Erdogan T. DFT, molecular docking and molecular dynamics simulation studies on some newly introduced natural products for their potential use against SARS-CoV-2. **J Mol Struct 2021**; 1242:130733.
48. Daina A, Michielin O, Zoete V. SwissADME: a free web tool to evaluate pharmacokinetics, drug-likeness and medicinal chemistry friendliness of small molecules. **Sci Rep 2017**; 7:42717.
49. Pires DE, Blundell TL, Ascher DB. pkCSM: predicting small-molecule pharmacokinetic and toxicity properties using graph-based signatures. **J Med Chem 2015**; 58(9): 4066−4072.
50. Lipinski CA, Lombardo F, Dominy BW, Feeney PJ. Experimental and computational approaches to estimate solubility and permeability in drug discovery and development settings. **Adv Drug Deliv Rev 1997**; 23(1−3): 3−25.
51. Veber DF, Johnson SR, Cheng H-Y, Smith BR, Ward KW, Kopple KD. Molecular properties that influence the oral bioavailability of drug candidates. **J Med Chem 2002**; 45(12): 2615−2623.
52. Muegge I, Oloff S. Advances in virtual screening. **Drug Discov Today Technol 2006**; 3(4): 405−411.
53. Clark DE. In silico prediction of blood−brain barrier permeation. **Drug Discov Today 2003**; 8(20): 927−933.

How to cite this article: Umar AB, Uzairu A. New flavone-based arylamides as potential *V600E-BRAF* inhibitors: Molecular docking, DFT, and pharmacokinetic properties. J Taibah Univ Med Sc 2023;18(5):1000−1010.